Global Elastic Response Simulation

Group Representative
Seiji Tsuboi Institute for Frontier Research on Earth Evolution

Author
Seiji Tsuboi Institute for Frontier Research on Earth Evolution

We simulate seismic waves propagating in three-dimensional (3-D) Earth model. There are two targets in this project; (1) to solve inverse problem, that is, to perform waveform inversion for 3-D shear wave velocity (Vs) structure inside the Earth using the Direct Solution Method and (2) to solve forward problem, that is, to calculate synthetic seismic waveform for fully 3-D Earth model. As for the inverse problem, we implement the codes of the Direct Solution Method on Earth Simulator to compute synthetic seismograms of long period surface waves and their partial derivatives with respect to model parameters of 3-D Earth structure. We perform waveform inversion for 3-D Vs structure and have improved the efficiency of the codes. As for the forward problem, we use the Spectral-Element Method and calculate synthetic seismic waveform for a 3-D Earth model, which includes a 3-D velocity and density structure, a 3-D crustal model, ellipticity as well as topography and bathymetry. We use 507 nodes of the Earth Simulator and show that we can calculate synthetic seismograms accurate up to 3.5 sec for global seismic network stations. We use seismograms recorded by about 600 high-gain short-period seismographic stations installed throughout Japan and have cross-correlated with synthetics calculated by SEM for a fully 3-D Earth model to read arrival times of seismic waves. We show that we can accurately measure the depths of the 410- and 660-km seismic velocity discontinuities in the Earth from these measurements.

Keywords: Synthetic seismograms, 3-D velocity structure of the Earth, Direct Solution Method, Spectral Element Method

1. Inverse Problem

We implement the codes of the Direct Solution Method on Earth Simulator to compute synthetic seismograms of long period surface waves and their partial derivatives with respect to model parameters of 3-D Earth structure. We use auto-parallelization of the compiler together with directives for parallel computing in a single node. We employ MPI to perform parallel calculation using multiple nodes.

We improve the computational efficiency of calculation of partial derivatives of synthetic seismograms with respect to model parameters of the Earth structure such as seismic velocity and density. This calculation is necessary to perform waveform inversion for the Earth structure. In the previous year, we performed waveform inversion for 3-D shear wave velocity structure in the depth range from 11 to 888 km. The number of waveforms used in inversion was 5110, and the horizontal resolution was about 1700 km. The parallelization ratio for calculation of partial derivatives, which is the most time-consuming, was 99.6%. In order to enlarge dataset and enhance the resolution of earth models, it is essential to improve the computational efficiency.

We follow Hara (2001) to increase the parallelization ratio. He suggested that it was possible to improve the computational efficiency by changing the order of model parameters and by equalizing computations assigned for each processor. We compare calculations using 5 and 10 nodes to find that the parallelization ratio become 99.82% by adopting his approach. Based on this result, we request 40 nodes, and obtain the parallelization ratio 99.92% based on comparison of the calculations using 20 and 40 nodes. This result suggests that it is possible to significantly improve the resolution of Earth models by application of the code developed this year.

2. Forward Problem

We use the spectral-element method (SEM) developed by Komatitsch and Tromp (2002) to simulate global seismic wave propagation throughout a 3-D Earth model, which includes a 3-D seismic velocity and density structure, a 3-D crustal model, ellipticity as well as topography and bathymetry. The SEM first divides the Earth into six chunks. Each of the six chunks is divided into slices. Each slice is allocated to one CPU of the Earth Simulator. Communication between each CPU is done by MPI. Before the system can be marched forward in time, the contributions from all the elements that share a common global grid point need to be summed. Since the global mass matrix is diagonal, time discretization of the second-order ordinary differential equation is achieved based upon a classical explicit second-order finite-difference scheme.

We could use 243 nodes (1944 CPUs) of the Earth Simulator by using the SEM last year. Using 243 nodes (1944 CPUs), we can subdivide six chunks into 1944 slices ($1944 = 6 \times 18 \times 18$). Each slice is then subdivided into 48 elements in one direction. Because each element has 5 Gauss-Lobatto Legendre integration points, then the average grid spacing at the surface of the Earth is about 2.9 km. The number of grid points in total amounts to about 5.5 billion. Using this mesh, it is expected that we can calculate synthetic seismograms accurate up to 5 sec all over the globe. We calculate synthetic seismograms for fully 3-D Earth model using the SEM code and 243 nodes of the ES for November 3, 2002 Alaska earthquake (Mw 7.9, depth 15.0 km). To simulate synthetic seismograms for this earthquake, we represent earthquake source by 475 point sources distributed both in space and time. The results of this simulation is summarized in Tsuboi et al (2003) and Komatitsch et al (2003), which was awarded 2003 Gordon Bell prize for peak performance in SC2003.

We then use 4056 processors, i.e., 507 nodes out of 640 of the Earth Simulator. Each slice is allocated to one processor of the Earth Simulator and subdivided with a mesh of 48×48 spectral-elements at the surface of each slice. Within each surface element we use $5 \times 5 = 25$ GLL grid points, which translates into an average grid spacing of 2.0 km (i.e., 0.018 degrees) at the surface. The total number of spectral elements in this mesh is 206 million, which corresponds to a total of 13.8 billion global grid points, since each spectral element contains $5 \times 5 \times 5 = 125$ grid points, but with points on its faces shared by neighboring elements. This in turn corresponds to 36.6 billion degrees of freedom (the total number of degrees of freedom is slightly less than 3 times the number of grid points because we solve for the three components of displacement everywhere in the mesh, except in the liquid outer core of the Earth where we solve for a scalar potential). Using this mesh, we can calculate synthetic seismograms that are accurate down to seismic periods of 3.5 seconds. This simulation uses a total of approximately 7 terabytes of memory. Total performance of the code, measured using the MPI Program Runtime Performance Information was 10 teraflops, which is about one third of expected peak performance for this number of nodes (507 nodes $\times$ 64 gigaflops = 32 teraflops). For the 243 nodes case, the total performance we achieved was about 5 teraflops, which also is about one third of the peak performance. The fact that when we double the number of nodes from 243 to 507 the total performance also doubles from 5 teraflops to 10 teraflops shows that this SEM code exhibits an excellent scaling relation with respect to performance. In Figure 1, we compare the vertical component of displacement from synthetic seismograms calculated using 507 nodes of the Earth Simulator and observed records for several broadband seismic stations of the F-net array operated by the National Institute of Earth Science and Disaster Prevention in Japan. The earthquake we calculated is a deep earthquake of magnitude 6.3 that occurred South of Japan on November 12, 2003, at a depth of 382 km. It is amazing that the global 3-D seismic velocity model used in this simulation still produces fairly good agreement with the observations even at periods of 3.5 seconds, because it is supposed that the crustal and mantle structure beneath Japanese Islands are highly heterogeneous and may be difficult to capture by using global 3D Earth model. However, Figure 1 also shows that the theoretical seismograms calculated with 507 nodes of the Earth Simulator do not reproduce some of the fine features in the observation and suggests the limitation of this global 3-D seismic velocity model. For those stations located to the north-east of the epicenter (the azimuth is about 20 degrees), the observed waves show large high-frequency oscillations because the waves travel along the subducting pacific plate, but this feature is not modeled in the theoretical seismograms. This shows that we need to improve our 3-D seismic wave velocity model to calculate theoretical seismic waves that are accurate at 3.5 seconds and longer.

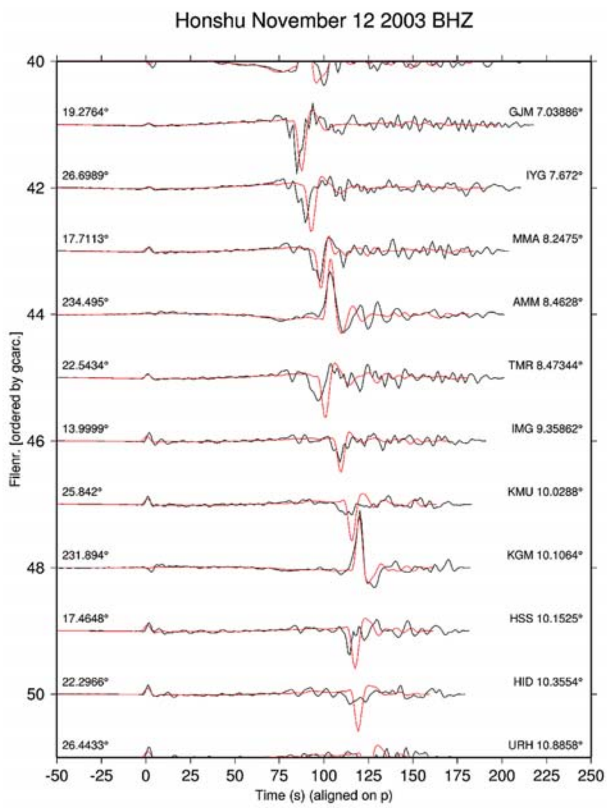

Fig. 1 Broadband data and synthetic displacement seismograms for the 2003 South of Honshu earthquake bandpass-filtered with a two-pass four-pole Butterworth filter between periods of 3.5 and 150 seconds. Vertical component data (black) and synthetic (red) displacement seismograms aligned on the arrival time of the P wave are shown. For each set of seismograms the azimuth is printed above the records to the left, and the station name and epicentral distance are printed to the right.

Next we show the results of Tono et al (2003). We use records of ~ 500 tiltmeters of the Hi-net, in addition to ~ 60 broadband seismometers of the F-net, operated by the National Research Institute for Earth Science and Disaster Prevention (NIED). We analyze pairs of sScS waves, which means S-wave traveled upward from the hypocenter reflected at the surface and reflected again at the core-mantle boundary, and its reverberation from the 410- or 660-km reflectors (sScSSdS where d = 410 or 660 km) for the deep shock of the Russia-N.E. China border (PDE; 2002:06:28; 17:19:30.30; 43.75N; 130.67E; 566 km depth; 6.7 Mb). The two horizontal components are rotated to obtain the transverse component. We have found that these records show clearly the near-vertical reflections from the 410- and 660-km seismic velocity discontinuities inside the Earth as postcursors of sScS phase. If we read the travel time difference between sScS and sScSSdS, we may say that this differential travel time anomaly can be attributed either to the local velocity anomaly along the SdS path or to the depth anomaly of the reflection point, because it is little affected by the uncertainties associated with the hypocentral determination, structural complexities near the source and receiver and long-wavelength mantle heterogeneity. The differential travel time anomaly is obtained by measuring the arrival time anomaly of sScS and that of sScSSdS separately and then by taking their difference. The arrival time anomaly of sScS (or sScSSdS) is measured by cross-correlating the observed sScS (or sScSSdS) with the corresponding synthetic waveform computed by SEM on the Earth Simulator. The sScSSdS signal is often severely contaminated by crustal reverberations, and this contamination is not simulated by wave synthetics with a laterally homogeneous crustal model, but in many cases it is accurately simulated by the SEM-synthetics incorporating 3-D crustal structure, topography and bathymetry. The correlation coefficients between the observed and SEM-synthetic sScS waveforms are in general higher than 0.8, and those for sScSSdS are in general higher than 0.6, with notable exceptions for stations in northern Japan where the waveform match is relatively poor. The synthesis by the SEM has resulted in a larger number of measured values of sScSSdS-sScS than the synthesis based on a laterally homogeneous Earth model. The observed differential travel time anomaly is relative to 3-D mantle model with long wavelength heterogeneity. The long-wavelength nature of this model makes it impossible to correct for local velocity anomalies along the SdS path to isolate the effect

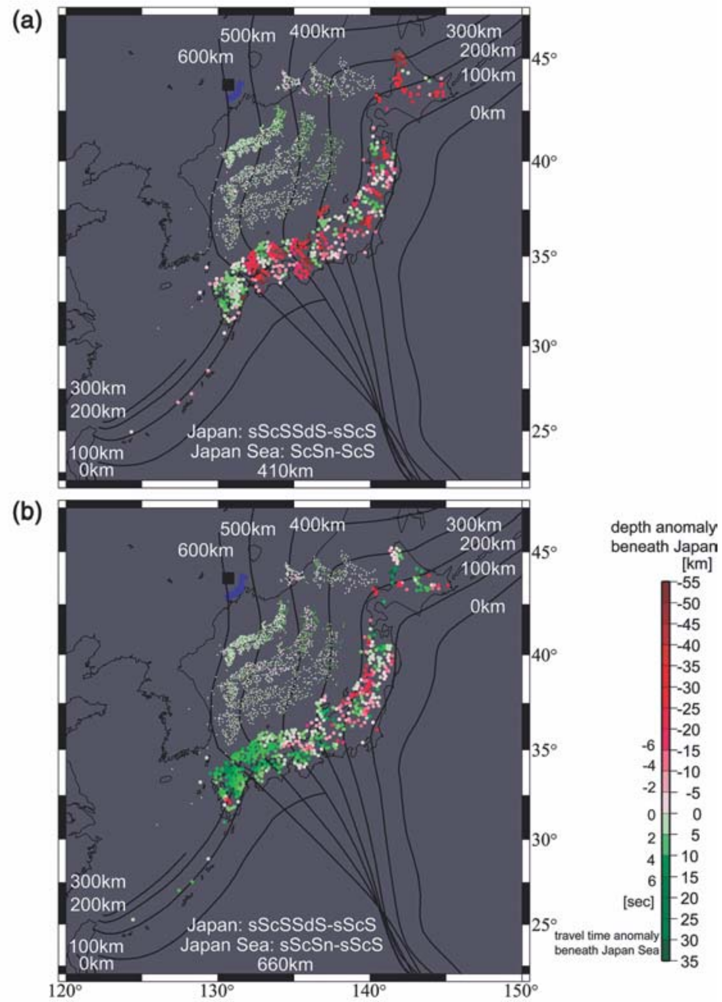

Fig. 2 Maps of the depth anomalies of the 410- (a) and the 660-km boundaries (b) beneath the Japanese islands. (From Tono et al, 2003) The anomaly values are indicated by the colors of the circles plotted at the reflection points of sScSSdS at depth d. The solid square represents the epicenter of the earthquake. Blue circles in a band near the epicenter indicate the reflection points of sSdSScS at 660-km depth. The isodepth contours of the Wadati-Benioff zone are also shown. The 400-km depth contour in southwestern Japan characterizes the depth anomaly patterns as described in the text. The numbers attached to the color scale refer, on the right, to the depth anomalies of the boundaries and, on the left, to the two-way travel time anomalies between the surface and core-mantle boundary from the ScSn-ScS data (a) and from the sScSn-sScS data (b), which are plotted at the corresponding surface bounce points in the Japan Sea.

due to reflection depth anomalies. An upper limit of the effect of the along-SdS velocity anomalies is given by the two-way near-vertical travel time anomaly between the core-mantle boundary (CMB) and the Earth's surface, which is obtained by measuring the differential travel times between ScS and its multiples ScSn and those between sScS and its multiples sScSn. Fig. 2 plots the measured values of the two-way near-vertical travel time anomaly (see the scale in sec) at the corresponding surface bounce points located beneath the Japan Sea. The values from ScSn-ScS and those from sScSn-sScS are shown respectively, showing consistently a small regional variation. These anomaly values are largely within ± 2 sec, while those of sScSSdS-sScS range from –20 to 15 sec. Such a contrast suggests that the effect of the along-SdS velocity anomaly is relatively small and that the sScSSdS-sScS anomalies are attributed mainly to the reflection depth anomaly. Ignoring the effect of the along-SdS velocity anomaly, the observed differential travel time anomalies of sScSSdS-sScS are converted to depth anomalies of SdS, using shear velocity and incident angle at the boundaries of 3-D mantle model. Figs. 2a and 2b plot the values of depth anomaly relative to the 410- and 660-km depths (see the scale in km), respectively, on the corresponding reflection points which are located beneath the Japanese Islands. Note that although the earthquake we used is just one, the number of the reflection points is enormous because of the very dense distribution of seismic stations. We also note that in contrast to the wide spread of the reflection points of sScSSdS which are located near the stations, those of sSdSScS (blue circles) are narrowly confined near the epicenter (black square) in a linear dimension comparable to the dominant wavelength of 200 km. This contrast is the reason why we have attributed the large lateral variation of the observed differential travel time anomalies to the one associated with sScSSdS rather than sSdSScS. The results show that the 660-km boundary is depressed at a constant level of ~15 km along the bottom of the horizontally extending aseismic slab under southwestern Japan. The transition from the normal to the depressed level occurs sharply, where the 660-km boundary intersects the bottom of the obliquely subducting slab. This observation should give important implications to geodynamic activities inside the Earth.

In summary, our SEM synthetics should provide unique way to reveal Earth's internal structure and earthquake source mechanisms in unprecedented resolution.

Acknowledgments

We used seismograms recorded at F-net and Hi-net stations operated by the National Institute of Earth Science and Disaster Prevention.

References

Hara, T., 2001. Improvement of the DSM computational efficiency to calculate partial derivatives of synthetic spectra with respect to model parameters of 3-D earth structure (abstract), Japan Earth planet. Sci. joint meeting 2001 meeting, http://www-jm.eps.s.u-tokyo.ac.jp/2001cd-rom/pdf/s4/s4-007_e.pdf.

D. Komatitsch, and J. Tromp, Spectral-element simulations of global seismic wave propagation-I. Validation. Geophys. J. Int. vol.149, pp.390–412, 2002.

D. Komatitsch, S. Tsuboi, C. Ji, and J. Tromp, A 14.6 billion degrees of freedom, 5 teraflops, 2.5 terabyte earthquake simulation on the Earth Simulator, Proceedings of the ACM/IEEE SC2003 confenrence, published on CD-ROM, 2003.

Y. Tono, T. Kunugi, Y. Fukao, S. Tsuboi, K. Kanjo, K. Kasahara, J. Tromp, and D. Komatitsch, Distribution of the 410- and 660-km boundaries by the subducted slab beneath Japan, Program. Abs. the Seismol. Soc. Japan 2003 Fall meeting, C062, 2003.

S. Tsuboi, D. Komatitsch, C. Ji, J. Tromp, Broadband modeling of the 2003 Denali fault earthquake on the Earth Simulator, Phys. Earth Planet. Int., vol.139, pp.305–312, 2003.